

Longitudinal response of three-body nuclei

R. Schiavilla and V. R. Pandharipande

Department of Physics, University of Illinois at Urbana-Champaign, Urbana, Illinois 61801

(Received 17 August 1987)

The method of correlated basis functions is generalized to describe three-nucleon and deuteron-plus-nucleon continuum states. The correlated basis functions are obtained by incorporating short range correlations between the spectator nucleon and the two nucleons of the interacting pair. Correlated orthonormal wave functions for the continuum states are generated by orthogonalizing the correlated basis functions via a combination of Schmidt and Löwdin transformations, designed so that the correlated orthonormal states have correct energies. The correlated orthonormal continuum states include the minimum interaction effects required to ensure orthogonality and reasonable short range behavior. The longitudinal response of ${}^3\text{He}$ and ${}^3\text{H}$ at $k=300$ to 600 MeV/c is calculated with the variational ground state wave function and the correlated orthonormal final states. Both the short range correlations and the orthogonality corrections in the final states decrease the response in the quasi-free peak. The calculated response has the correct sum and energy-weighted sum within $\sim 5\%$, and that of ${}^3\text{He}$ is in reasonable agreement with the Saclay experimental data. We find that the response of ${}^3\text{H}$ is broader than that of ${}^3\text{He}$, and that it is relatively larger at energies greater than that of the quasi-free peak.

I. INTRODUCTION

In recent years there have been many measurements¹⁻⁵ of the longitudinal and transverse response of light, medium, and heavy nuclei by inclusive electron scattering. It is hoped that the longitudinal response function is not significantly affected by meson exchange currents involving pion and delta electroproduction,⁶ and therefore it provides a test for our understanding of the nuclear wave function, and of the coupling of nucleons in nuclei to the electromagnetic field.^{7,8}

The three-body nuclei ${}^3\text{He}$ and ${}^3\text{H}$ are of particular interest because their ground state wave functions can be calculated rather accurately, from realistic nuclear Hamiltonians, with Faddeev⁹ or variational¹⁰ methods. From these ground state wave functions we have earlier calculated the sum¹¹ $S_L(k)$ and the energy weighted sum¹² $W_L(k)$ of the longitudinal response function $S_L(k, \omega)$. These sums are within $\sim 5\%$ of those obtained from the experimental data¹ on ${}^3\text{He}$.

It is much harder to calculate $S_L(k, \omega)$ because that requires the wave functions of the three-nucleon continuum states. The recent calculations^{13,14} of $S_L(k, \omega)$ do not fit the experimental data very well. The calculated $S_L(k, \omega)$ is $\sim 20-30\%$ larger than the experimental in the region of the quasi-elastic peak. This discrepancy was attributed in Ref. 13 to the weakness of a theoretical picture of the quasi-elastic process based on the plane-wave-impulse approximation (PWIA). The PWIA description was improved by Laget,¹⁴ whose included, in an approximate way, the final state interactions due to rescattering of the knocked-out nucleon. However, the discrepancy of $\sim 20\%$ still remained.

In this paper we calculate the longitudinal response

functions of ${}^3\text{He}$ and ${}^3\text{H}$ at momentum transfers $k=300, 400, 500,$ and 600 MeV/c using correlated orthogonal final states.

We first generalize the correlated basis functions (CBF) approach to describe the three-nucleon continuum states. The CBF method was initially developed in the theory of quantum liquids,¹⁵ and the correlated orthogonal states were recently used to study the response of nuclear matter.¹⁶

In the purely pedagogical Sec. II we use the correlated orthogonal states theory to show that it can give a qualitative description of the nucleon-nucleon scattering even in the lowest order Born approximation. The correlated two-nucleon states are obtained by operating, on the plane wave states, by a two-body correlation operator.

In Sec. III correlated three-nucleon continuum states of the type $d + N$ and $3N$ are constructed by acting with correlation operators on a wave function having an interacting pair of nucleons or a deuteron and a spectator nucleon in a plane wave. Correlated orthogonal (CO) states are constructed from these by antisymmetrization and by the Schmidt-Löwdin orthogonalization procedure developed in Ref. 16. The problems of nonorthogonality of the continuum and bound states, in intermediate energy nuclear reactions, have been discussed earlier in the literature.^{17,18}

The CO states are used to calculate the longitudinal response in first order perturbation theory in Sec. IV. It is shown that both the short range correlations and the orthogonality corrections reduce the height of the peak of $S_L(k, \omega)$ of ${}^3\text{He}$, and bring it into reasonable agreement with experiment. The results for both ${}^3\text{He}$ and ${}^3\text{H}$ are presented in Sec. V, and the conclusions are summarized in Sec. VI. Most of the calculational details are given in Appendices so that the text is easy to read.

II. CORRELATED BASIS THEORY OF NN SCATTERING

The CBF for two-nucleon states has the form

$$\psi_{\mathbf{k}\alpha\beta}(\mathbf{r}_{12}) = F_{12} A \frac{1}{\sqrt{\Omega}} e^{i\mathbf{k}\cdot\mathbf{r}_{12}} \chi_{\alpha}(1) \chi_{\beta}(2), \quad (2.1)$$

where \mathbf{k} is the relative momentum, α and β specify the spin-isospin states, $\mathbf{r}_{12} = \mathbf{r}_1 - \mathbf{r}_2$, F_{12} is the correlation

operator, A is the antisymmetrization operator, and Ω is the normalization volume. F_{12} takes into account short-range correlations in the wave function, and we require that

$$F_{12}(r_{12} > d) = 1. \quad (2.2)$$

In the present work we take it as a sum of six terms:

$$F_{12} = \sum_{p=1,6} f^p(r_{12}) O_{12}^p, \quad (2.3)$$

$$O_{12}^p = 1, \tau_1 \cdot \tau_2, \sigma_1 \cdot \sigma_2, \tau_1 \cdot \tau_2 \sigma_1 \cdot \sigma_2, S_{12}, \text{ and } \tau_1 \cdot \tau_2 S_{12}, \quad (2.4)$$

where S_{12} is the tensor operator. The F_{12} used in nuclear-matter theory¹⁹ also contains spin-orbit correlations which are neglected here for simplicity. The condition (2.2) implies that the $f^p = 1(r_{12} > d) = 1$, while all $f^p > 1(r_{12} > d) = 0$. We use the F_{12} developed for nuclear-matter theory as discussed in Appendix A.

The correlated basis states (2.1) are denoted by $|\mathbf{k}\alpha\beta\rangle$. They are not orthonormal:

$$\langle \mathbf{k}'\alpha'\beta' | \mathbf{k}\alpha\beta \rangle = \delta_{\mathbf{k}\mathbf{k}'} \delta_{\alpha\alpha'} \delta_{\beta\beta'} - \delta_{\mathbf{k}-\mathbf{k}'} \delta_{\alpha\beta'} \delta_{\beta\alpha'} + \text{terms of order } 1/\Omega. \quad (2.5)$$

We orthogonalize them with the Löwdin²⁰ transformation to obtain CO states:

$$|\mathbf{k}\alpha\beta\rangle = |\mathbf{k}\alpha\beta\rangle - \frac{1}{2} |\mathbf{k}'\alpha'\beta'\rangle \langle \mathbf{k}'\alpha'\beta' | \mathbf{k}\alpha\beta \rangle + \frac{3}{8} |\mathbf{k}''\alpha''\beta''\rangle \langle \mathbf{k}''\alpha''\beta'' | \mathbf{k}'\alpha'\beta' \rangle \langle \mathbf{k}'\alpha'\beta' | \mathbf{k}\alpha\beta \rangle - \dots \quad (2.6)$$

The coefficients $1, -\frac{1}{2}, +\frac{3}{8}, \dots$ of the terms in this transformation are those that occur in the Taylor expansion of $(1+x)^{-1/2}$; there is a sum over all repeated quantum numbers $\mathbf{k}'\alpha'\beta' \dots$, and a bar over a matrix element implies that the diagonal terms are to be omitted. The CO states are denoted $|\mathbf{k}\alpha\beta\rangle$, whereas the correlated but not orthogonal CBF states are denoted $|\mathbf{k}\alpha\beta\rangle$.

The correlated basis theory is a perturbation theory in which the CO states are used instead of plane-wave states having $F_{12} = 1$. When the interaction is strong, perturbation theory with plane-wave states has a poor convergence, and, in particular, the Born approximation

is meaningless. However, we hope that, with an appropriate choice of F_{12} , the correlated basis theory has a reasonable convergence. Most of the present work uses only the first order, i.e., the Born approximation, in correlated basis theory.

The Hamiltonian is given by

$$H = -\frac{\hbar^2}{m} \nabla_{12}^2 + v_{12}, \quad (2.7)$$

where v_{12} is the two-nucleon interaction. The Argonne²¹ v_{14} interaction is used in this work. The matrix elements of the Hamiltonian with CO states are given by

$$\begin{aligned} \langle \mathbf{k}'\alpha'\beta' | H | \mathbf{k}\alpha\beta \rangle &= \langle \mathbf{k}'\alpha'\beta' | H | \mathbf{k}\alpha\beta \rangle - \frac{1}{2} \langle \mathbf{k}'\alpha'\beta' | H | \mathbf{k}''\alpha''\beta'' \rangle \langle \mathbf{k}''\alpha''\beta'' | \mathbf{k}\alpha\beta \rangle \\ &\quad - \frac{1}{2} \langle \mathbf{k}'\alpha'\beta' | \mathbf{k}''\alpha''\beta'' \rangle \langle \mathbf{k}''\alpha''\beta'' | H | \mathbf{k}\alpha\beta \rangle + \dots \end{aligned} \quad (2.8)$$

The diagonal CBF matrix elements $\langle \mathbf{k}\alpha\beta | H | \mathbf{k}\alpha\beta \rangle$ and $\langle \mathbf{k}\alpha\beta | \mathbf{k}\alpha\beta \rangle$ are of order 1, while the nondiagonal elements $\langle \mathbf{k}'\alpha'\beta' | H | \mathbf{k}\alpha\beta \rangle$ and $\langle \mathbf{k}'\alpha'\beta' | \mathbf{k}\alpha\beta \rangle$ are of order $1/\Omega$.

Let us consider the diagonal element of H in CO states. It is easy to see that

$$\langle \mathbf{k}\alpha\beta | H | \mathbf{k}\alpha\beta \rangle = \frac{\hbar^2}{m} k^2 + \text{terms of order } 1/\Omega. \quad (2.9)$$

In the limit $\Omega \rightarrow \infty$ this matrix element is exact, only the first term in Eq. (2.8) gives the finite contribution, and

the rest can be neglected. On the other hand, the nondiagonal matrix elements of H are of order $1/\Omega$, and every term in Eq. (2.8) has a contribution of order $1/\Omega$. Thus, in principle, the series (2.8) has to be summed to obtain the nondiagonal matrix elements of H . In most cases this series converges quite rapidly, and it is possible to sum it, as discussed in Sec. IV.

In the Born approximation calculation of NN scattering in correlated basis theory, we need only the nondiagonal matrix elements of H for $|\mathbf{k}'| = |\mathbf{k}|$. These can be more conveniently calculated as follows:

$$\begin{aligned}
\langle \mathbf{k}'\alpha'\beta' | H | \mathbf{k}\alpha\beta \rangle &= \left\langle \mathbf{k}'\alpha'\beta' \left| H - \frac{\hbar^2}{m} k^2 \right| \mathbf{k}\alpha\beta \right\rangle \\
&= \left[\mathbf{k}'\alpha'\beta' \left| H - \frac{\hbar^2}{m} k^2 \right| \mathbf{k}\alpha\beta \right] - \frac{1}{2} \left[\mathbf{k}'\alpha'\beta' \left| H - \frac{\hbar^2}{m} k^2 \right| \mathbf{k}''\alpha''\beta'' \right] (\overline{\mathbf{k}''\alpha''\beta'' | \mathbf{k}\alpha\beta}) \\
&\quad - \frac{1}{2} (\overline{\mathbf{k}'\alpha'\beta' | \mathbf{k}''\alpha''\beta''}) \left[\mathbf{k}''\alpha''\beta'' \left| H - \frac{\hbar^2}{m} k^2 \right| \mathbf{k}\alpha\beta \right] + \cdots .
\end{aligned} \tag{2.10}$$

This series has a better convergence than (2.8). In the present calculation, meant primarily to illustrate the method, we simply keep the first term in Eq. (2.10) and neglect the rest. In a more serious calculation one might have to sum the first few terms of Eq. (2.10), and also Schmidt-orthogonalize the states $|\mathbf{k}\alpha\beta\rangle$ to the deuteron, as discussed in the next section.

In the correlated basis Born approximation (CBBA) the T matrix is given by

$$T^{(1)}(\mathbf{k}'\alpha'\beta', \mathbf{k}\alpha\beta) = \langle \mathbf{k}'\alpha'\beta' | H | \mathbf{k}\alpha\beta \rangle . \tag{2.11}$$

Further details of the calculation are given in Appendix B. Both the exact and CBBA cross sections shown in Figs. 1–6 are obtained by retaining only the partial waves having $j \leq 5$ in the expansion of the T matrix. We note that, unlike the plane-wave Born approximation (PWBA), which gives meaningless results for NN scattering with realistic interactions, the cross sections obtained with the CBBA are quite reasonable. This is because a bulk of the effects of higher order terms, such as the reduction of the wave function in the region of the repulsive core, the coupling to other channels due to tensor forces, etc., are already included in the first order CBBA via the correlation operators.

Figures 1–6 do not show the “best possible” CBBA results. We have used an F_{12} from the theory of nuclear matter, and it may be possible to develop a better F_{12} for NN scattering. Furthermore, inclusion of spin-orbit correlations will improve the results at higher energies.

III. THREE-BODY CORRELATED ORTHOGONAL STATES

Correlated basis functions for the three-body continuum states are written as

$$\begin{aligned}
\psi_{\mathbf{q}\alpha, E_2\gamma} &= \frac{1}{\sqrt{3}} \sum_{\text{cyc}} \frac{1}{2} \{ F_{ij}, F_{ik} \} \frac{1}{\sqrt{\Omega}} \\
&\quad \times e^{i\mathbf{q}\cdot(\mathbf{r}_i - \mathbf{R}_{jk})} \chi_{\alpha}(i) \phi_{E_2\gamma}(jk) ,
\end{aligned} \tag{3.1}$$

where α specifies the spin-isospin of the “spectator” nucleon and γ denotes the spin-isospin $lsjm_j m_t$ of “the pair.” The $\phi_{E_2\gamma}(jk)$ is an antisymmetric eigenfunction of the two-body Hamiltonian (2.7) with energy E_2 . Thus $\phi(jk)$ contains correlations between j and k . The correlations of i with j and k are described with the symmetrized product of F_{ij} and F_{ik} . Note that the F_{ij} and F_{ik} do not generally commute. The cyclic sum in (3.1) is

over particle indices i, j , and k . Since $\phi(ij)$ is antisymmetric under the exchange of i with j , the cyclic sum ensures that the CBF (3.1) is antisymmetric. The factor $1/\sqrt{3}$ is for normalization, and $\mathbf{R}_{jk} = \frac{1}{2}(\mathbf{r}_j + \mathbf{r}_k)$.

The three-body states include the bound states denoted $|1, M_S M_T\rangle$, where $M_T = \pm \frac{1}{2}$ for ${}^3\text{He}$ and ${}^3\text{H}$, respectively. In our notation $|n, Q\rangle$ denotes a CBF with n clusters and quantum numbers Q . The $|1, M_S M_T\rangle$ are either Faddeev⁹ or variational¹⁰ ground state wave functions. The deuteron and nucleon (d + N) states $\psi_{\mathbf{q}\alpha, M_d}$ (M_d is the deuteron spin projection) are denoted $|2, \mathbf{q}\alpha M_d\rangle$. They are obtained by replacing $\phi_{E_2\gamma}(jk)$ in Eq. (3.1) with the deuteron wave function $\phi_{M_d}(jk)$. The states with three nucleons in the continuum (3N states), given by Eq. (3.1), are denoted $|3, \mathbf{q}\alpha E_2\gamma\rangle$ with $E_2 > 0$.

The correlated states $|n, Q\rangle$ have correct diagonal elements of H (the energies) in the limit $\Omega \rightarrow \infty$. $(1, Q | H | 1, Q)$ is simply the energy of the ${}^3\text{He}$ or ${}^3\text{H}$ nucleus, and it can be verified that

$$\begin{aligned}
(2, \mathbf{q}\alpha M_d | H | 2, \mathbf{q}\alpha M_d) \\
= \frac{3\hbar^2}{4m} q^2 + E_d + \text{terms of order } 1/\Omega ,
\end{aligned} \tag{3.2}$$

$$\begin{aligned}
(3, \mathbf{q}\alpha E_2\gamma | H | 3, \mathbf{q}\alpha E_2\gamma) \\
= \frac{3\hbar^2}{4m} q^2 + E_2 + \text{terms of order } 1/\Omega .
\end{aligned} \tag{3.3}$$

However, $|n, Q\rangle$ are not orthogonal to each other even when $F_{12} = 1$. It is not desirable to orthogonalize all the states $|n, Q\rangle$ by a single Löwdin transformation,

$$|n, Q\rangle = |n, Q\rangle - \frac{1}{2} |n', Q'\rangle (\overline{n', Q' | n, Q}) + \cdots , \tag{3.4}$$

because the states obtained this way do not have the correct energies. As an example, consider the energy of the state $|1, Q\rangle$ obtained from (3.4),

$$\begin{aligned}
\langle 1, Q | H | 1, Q \rangle &= (1, Q | H | 1, Q) \\
&\quad - \frac{1}{2} [(1, Q | H | n', Q') \\
&\quad \quad \times (\overline{n', Q' | 1, Q}) + \text{c.c.}] \\
&\quad + \cdots .
\end{aligned} \tag{3.5}$$

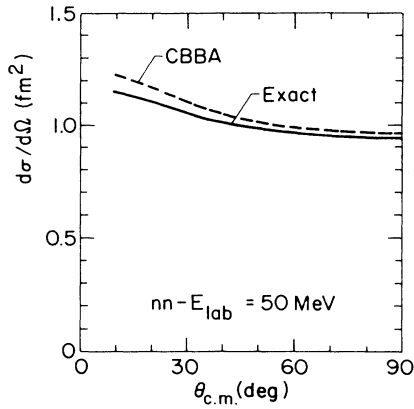


FIG. 1. The exact and CBBA n-n scattering differential cross section at $E_{\text{lab}} = 50$ MeV.

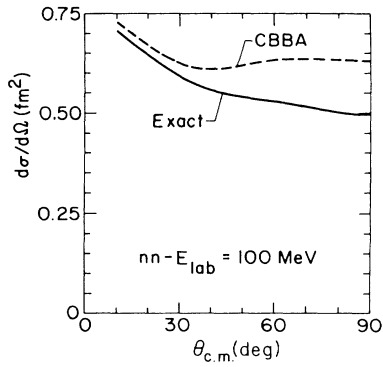


FIG. 2. The exact and CBBA n-n scattering differential cross section at $E_{\text{lab}} = 100$ MeV.

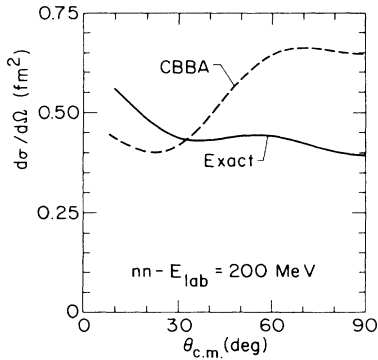


FIG. 3. The exact and CBBA n-n scattering differential cross section at $E_{\text{lab}} = 200$ MeV.

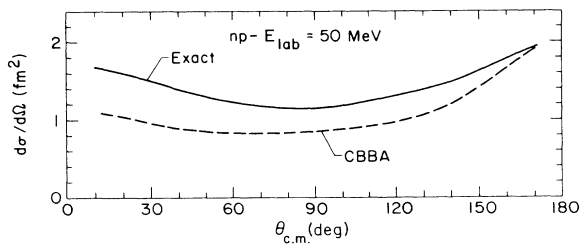


FIG. 4. The exact and CBBA n-p scattering differential cross section at $E_{\text{lab}} = 50$ MeV.

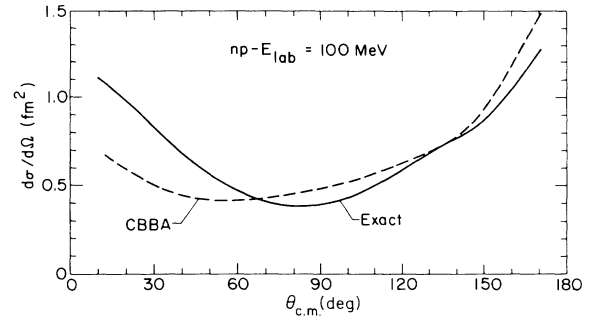


FIG. 5. The exact and CBBA n-p scattering differential cross section at $E_{\text{lab}} = 100$ MeV.

The first term $\langle 1, Q | H | 1, Q \rangle$ gives the correct energy; however, the subsequent terms of (3.5) are not negligible, and they destroy the correct energy of the correlated state $|1, Q\rangle$. To see this, consider the terms with $n' = 2$. The matrix elements $\langle 2, Q' | 1, Q \rangle$ and $\langle 1, Q | H | 2, Q' \rangle$ are each order $1/\sqrt{\Omega}$; however, the number of $|2, Q'\rangle$ states is of order Ω , and hence the second term of (3.5) gives an unwanted finite contribution even in the limit $\Omega \rightarrow \infty$.

A similar problem also occurs in the correlated basis theories of quantum liquids. If all the correlated states are orthogonalized by a single Löwdin transformation, their energies are spoiled. Techniques to orthogonalize states while preserving diagonal elements of the Hamiltonian were developed to calculate the response of nuclear matter.¹⁶ These same techniques can be used here to orthogonalize the states $|n, Q\rangle$ while preserving their energies.

The states $|1, Q\rangle$ are orthogonal to each other, and we identify

$$|1, Q\rangle = |1, Q\rangle. \quad (3.6)$$

The correlated orthogonal states $|1, Q\rangle$ obviously have correct energies provided the Faddeev or a good variational ground state wave function is used. Next, we define a set of intermediate states

$$|2, Q\rangle = |2, Q\rangle - |1, Q'\rangle \langle 1, Q' | 2, Q\rangle. \quad (3.7)$$

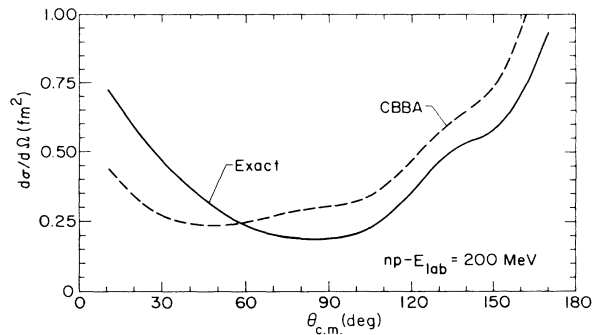


FIG. 6. The exact and CBBA n-p scattering differential cross section at $E_{\text{lab}} = 200$ MeV.

These states are orthogonalized to $|1, Q'\rangle$ by the Schmidt procedure, and they have correct energies in the limit $\Omega \rightarrow \infty$, since both $\langle 1, Q' | H | 2, Q \rangle$ and $\langle 1, Q' | 2, Q \rangle$ are of order $1/\sqrt{\Omega}$, and there is a finite number of states $|1, Q\rangle$. The CO states $|2, Q\rangle$ are obtained by orthogonalizing the states $|2, Q\rangle$ among themselves by a Löwdin transformation;

$$|2, Q\rangle = |2, Q\rangle - \frac{1}{2} |2, Q'\rangle \overline{\langle 2, Q' | 2, Q \rangle} + \dots \quad (3.8)$$

This transformation does not change the energies of these states in the limit $\Omega \rightarrow \infty$ because both $\langle 2, Q | H | 2, Q'\rangle$ and $\langle 2, Q | 2, Q'\rangle$ are of order $1/\Omega$.

The CO states $|3, Q\rangle$ are obtained in a similar way:

$$|3, Q\rangle = |3, Q\rangle - |1, Q'\rangle \langle 1, Q' | 3, Q \rangle - |2, Q'\rangle \langle 2, Q' | 3, Q \rangle, \quad (3.9)$$

$$|3, Q\rangle = |3, Q\rangle - \frac{1}{2} |3, Q'\rangle \overline{\langle 3, Q' | 3, Q \rangle} + \dots \quad (3.10)$$

It can be verified that these states are orthogonal, and that they have correct normalization and energies in the limit $\Omega \rightarrow \infty$. They, however, are not eigenstates of H , but we can hope that perturbation theory has a good convergence in the basis of these states.

IV. CALCULATION OF LONGITUDINAL RESPONSE

In a theory in which only the nucleon degrees of freedom are retained, the longitudinal response is given by

$$S_L(k, \omega, M_T) = \frac{1}{2} \sum_{M_S} \sum_{n=2,3} \sum_Q |\langle n, Q | e^{-ik \cdot R} \rho_{p,k} | 1, M_S M_T \rangle|^2 \delta(\omega + E_0(M_T) - E(n, Q)) \quad (4.6)$$

$$\equiv \sum_{n=2,3} S_L(k, \omega, M_T, n). \quad (4.7)$$

The contribution of d + N states is given by

$$S_L(k, \omega, M_T, 2) = \frac{1}{2} \sum_{M_S} \sum_{M_d \sigma_z} \int \frac{d\mathbf{q}}{(2\pi)^3} |A(\mathbf{q}, \sigma_z M_d M_S)|^2 \delta(\omega + E_0(M_T) - E(2, q^2)), \quad (4.8)$$

$$A(\mathbf{q}, \sigma_z M_d M_S) \equiv \langle 2, \mathbf{q} \sigma_z (\tau_z = M_T) M_d | e^{-ik \cdot R} \rho_{p,k} | 1, M_S M_T \rangle. \quad (4.9)$$

Note that since the deuteron has zero isospin, the τ_z of the spectator nucleon must be equal to that of the target (M_T). Using Eq. (3.8) for $|2, Q\rangle$, we obtain

$$A(\mathbf{q}, \sigma_z M_d M_S) = \sum_{i=0, \infty} (-1)^i \frac{(2i-1)!!}{2^i i!} A_i(\mathbf{q}, \sigma_z M_d M_S), \quad (4.10)$$

$$A_0(\mathbf{q}, \sigma_z M_d M_S) \equiv \langle 2, \mathbf{q} \sigma_z M_d | e^{-ik \cdot R} \rho_{p,k} | 1, M_S M_T \rangle, \quad (4.11)$$

$$A_i(\mathbf{q}, \sigma_z M_d M_S) = \sum_{\sigma'_z M'_d} \int \frac{d\mathbf{q}'}{(2\pi)^3} \overline{\langle 2, \mathbf{q}' \sigma'_z M'_d | 2, \mathbf{q}' \sigma'_z M'_d \rangle} A_{i-1}(\mathbf{q}', \sigma'_z M'_d M_S). \quad (4.12)$$

In Eq. (4.10), $(-1)!!$ is to be taken as 1. The A_0 can be trivially expressed in terms of matrix elements with correlated states. Using Eqs. (3.6) and (3.7), we obtain

$$A_0(\mathbf{q}, \sigma_z M_d M_S) = \langle 2, \mathbf{q} \sigma_z M_d | e^{-ik \cdot R} \rho_{p,k} | 1, M_S M_T \rangle - \langle 2, \mathbf{q} \sigma_z M_d | 1, M_S M_T \rangle \langle 1, M_S M_T | e^{-ik \cdot R} \rho_{p,k} | 1, M_S M_T \rangle \quad (4.13)$$

$$= \langle 2, \mathbf{q} \sigma_z M_d | e^{-ik \cdot R} \rho_{p,k} - F_{el}(\mathbf{k}, M_S M_T) | 1, M_S M_T \rangle, \quad (4.14)$$

$$R_L(\mathbf{k}, \omega) = |G_E(k, \omega)|^2 S_L(\mathbf{k}, \omega), \quad (4.1)$$

$$S_L(\mathbf{k}, \omega) = \sum_I |\langle I | \rho_{p,k} | 0 \rangle|^2 \delta(\omega + E_0 - E_I), \quad (4.2)$$

$$\rho_{p,k} = \sum_{i=1, A} e^{ik \cdot \mathbf{r}_i} \frac{1}{2} [1 + \tau_3(i)]. \quad (4.3)$$

Here, $|0\rangle$ denotes the ground state of the target with energy E_0 , $|I\rangle$ are the eigenstates of the nuclear Hamiltonian with energies E_I , and—by convention—the recoiling ground state from elastic scattering is omitted in the sum over I . In the present work we have used the covariant proton form factor:

$$G_E(k, \omega) = \left[1 + \frac{k^2 - \omega^2}{(833.88 \text{ MeV})^2} \right]^{-2}, \quad (4.4)$$

which gives a fairly accurate description of free electron-proton scattering.²²

In the lowest order of correlated basis theory the correlated orthogonal states discussed in the preceding section are used in place of the states $|I\rangle$ to calculate the response. Higher order corrections take into account the difference between the states $|I\rangle$ and CO states $|n, Q\rangle$. They are discussed in Ref. 16, but not considered here. The CO states with total momentum \mathbf{k} are obtained by multiplying the zero total momentum states of Sec. III by $e^{ik \cdot \mathbf{R}}$, where

$$\mathbf{R} = \frac{1}{3} (\mathbf{r}_1 + \mathbf{r}_2 + \mathbf{r}_3), \quad (4.5)$$

and we have set $\Omega = 1$. Thus the lowest order response is obtained as

where $F_{el}(\mathbf{k}, M_S M_T)$ is the elastic scattering form factor. In general, Schmidt orthogonalization of the excited states to the ground state results in replacing $e^{-i\mathbf{k}\cdot\mathbf{R}}\rho_{p,k}$ by $e^{-i\mathbf{k}\cdot\mathbf{R}}\rho_{p,k} - F_{el}(\mathbf{k})$, and it significantly reduces the calculated $S_L(k, \omega)$.

Most of the details of the calculation of the response are given in Appendix C. Here we briefly comment on the importance of various terms and the approximations made in the calculation. Figure 7 is meant to illustrate the effect of the correlations $\{F_{ij}, F_{ik}\}$ in the final state [Eq. (3.1)]. It shows the longitudinal response of ${}^3\text{He}$ at $k = 400 \text{ MeV}/c$ calculated with uncorrelated final states ($F=1$) and correlated basis states $|n, Q\rangle$. None of the orthogonality corrections are included in obtaining the response shown in Fig. 7. We note from this figure that the short range correlations in the final states reduce the response by $\sim 10\%$.

The effects of orthogonalizing the correlated states are shown in Fig. 8. The curves labeled GSO (denoting ground state orthogonalization) are obtained by replacing the $e^{-i\mathbf{k}\cdot\mathbf{R}}\rho_{p,k}$ by $e^{-i\mathbf{k}\cdot\mathbf{R}}\rho_{p,k} - F_{el}(\mathbf{k})$ in the calculation of the response. Thus these curves show the effect of orthogonalizing the final states to the recoiling ground

state. This correction also reduces the response by $\sim 10\%$, and hence it is as important as the short range correlations.

The curve GSO(dp) in Fig. 8 shows the contribution of the $d + p$ states to the response in the approximation

$$A(\mathbf{q}, \sigma_z M_d M_S) \sim A_0(\mathbf{q}, \sigma_z M_d M_S).$$

Further corrections to it come from the orthogonalization of the $d + p$ states among themselves by the Löwdin transformation (3.8). These Löwdin corrections are given by the terms $A_{i \geq 1}(\mathbf{q}, \sigma_z M_d M_S)$ [Eq. (4.12)]. They are quite small as shown in Fig. 8, and we simplify their calculation significantly by calculating the kernel $\{2, \mathbf{q}\sigma_z M_d | 2, \mathbf{q}'\sigma'_z M'_d\}$ in the approximation $F=1$.

The $3N$ states $|3, Q\rangle$ used to calculate $S_L(k, \omega, M_T, 3)$ have quantum numbers

$$Q = \mathbf{q}\sigma_z \tau_z, \text{ } p l s j m_j t m_t, \quad (4.15)$$

where $\mathbf{q}\sigma_z \tau_z$ specify the "spectator," $l s j m_j t m_t$ give the angular momentum, spin, and isospin of the "pair," and the energy E_2 of the pair is $\hbar^2 p^2 / m$. We have neglected the Löwdin corrections in the calculation of $S_L(k, \omega, M_T, 3)$ by approximating:

$$\langle 3, Q | e^{-i\mathbf{k}\cdot\mathbf{R}}\rho_{p,k} | 1, M_S M_T \rangle \approx \langle 3, Q | e^{-i\mathbf{k}\cdot\mathbf{R}}\rho_{p,k} | 1, M_S M_T \rangle \quad (4.16)$$

$$= \langle 3, Q | e^{-i\mathbf{k}\cdot\mathbf{R}}\rho_{p,k} - F_{el}(\mathbf{k}) | 1, M_S M_T \rangle$$

$$- \sum_{\sigma'_z M'_d} \int \frac{d\mathbf{q}'}{(2\pi)^3} \langle 3, Q | 2, \mathbf{q}'\sigma'_z M'_d \rangle \langle 2, \mathbf{q}'\sigma'_z M'_d | e^{-i\mathbf{k}\cdot\mathbf{R}}\rho_{p,k} | 1, M_S M_T \rangle. \quad (4.17)$$

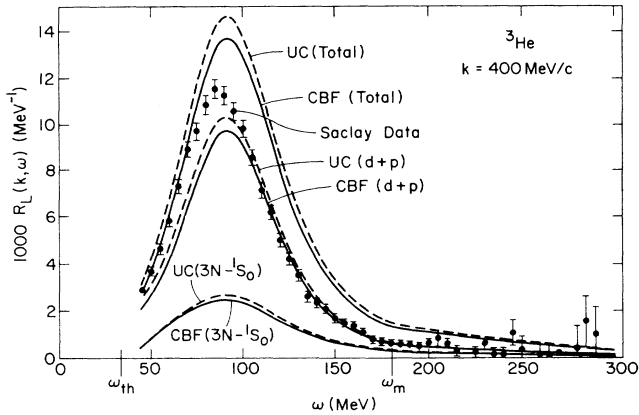


FIG. 7. The ${}^3\text{He}$ longitudinal response at $k = 400 \text{ MeV}/c$ obtained with the CBF states $|n, Q\rangle$ are shown by solid lines. The curves labeled total, $d + p$, and $3N-{}^1S_0$, respectively, give the total response, and the contributions of $d + p$ states and $3N$ states with $l s j = {}^1S_0$. The dashed curves labeled UC give the results obtained upon neglecting the correlations between the spectator and the interacting pair by setting $F=1$. ω_{th} and ω_m mark the energies for the $d + p$ threshold and the maximum energy up to which the response is calculated. The points with error bars show the observed response from Ref. 1.

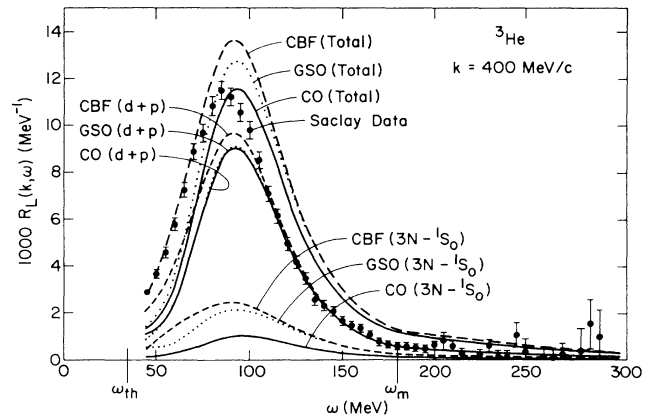


FIG. 8. The curves labeled CBF (dashed), GSO (dotted), and CO (solid lines) show the response obtained with the CBF states $|n, Q\rangle$, with states obtained by orthogonalizing the CBF states to the ground state, and with the correlated orthogonal states. See caption of Fig. 7 for other details.

Of all the three-nucleon continuum states, those with two particles (the "pair") in a 1S_0 state give the largest contribution. This contribution is shown in Fig. 8 with various approximations. We see that orthogonalizing the 3N continuum states to the d + N states has a large effect on the response, while orthogonalization to the ground state has a smaller but significant effect.

The energies of the final states, as calculated with non-relativistic kinematics in the lab frame, are

$$E_{\text{NR}} = \frac{\hbar^2 k^2}{6m} + \frac{3\hbar^2 q^2}{4m} + E_2, \quad (4.18)$$

where $E_2 = E_d$ for d + N states and $E_2 = \hbar^2 p^2/m$ for 3N states. It may be more accurate to calculate the final state energies with relativistic kinematics. They are

$$E_{\text{RK}} = \left[\hbar^2 \left(\frac{\mathbf{k}}{3} + \mathbf{q} \right)^2 + m^2 \right]^{1/2} + \left[\hbar^2 \left(\frac{2\mathbf{k}}{3} - \mathbf{q} \right)^2 + M_2^2 \right]^{1/2} - 3m, \quad (4.19)$$

where M_2 is the deuteron mass for d + N states and $M_2 = 2(m^2 + p^2)^{1/2}$ for 3N states. The responses shown in Figs. 7 and 8 are obtained with E_{NR} , while the response obtained with E_{RK} is compared with experiment and the results of NR calculations in Fig. 9. We see that the presumably more accurate calculation using relativistic kinematics is in slightly better agreement with the experimental data. The results shown in all subsequent figures are obtained with the E_{RK} .

In principle, one has to sum over all values of lsj to calculate the contribution of 3N states to the response. In practice, this sum has to be truncated. We have taken a somewhat pragmatic approach to this problem. We know the total integral,

$$\frac{1}{Z} \int_{\omega_{\text{el}}}^{\infty} S_L(k, \omega) d\omega \equiv S_L(k), \quad (4.20)$$

where Z is the charge of the target, from the ground state calculations.¹¹ Any calculation of $S_L(k, \omega)$ which

uses the correct ground state wave function and a complete orthonormal set of final states must reproduce the $S_L(k)$.

The 3N states with $lsj = ^1S_0$ give a large contribution, while states with other lsj values give relatively small contributions that are expected to add up to a contribution of the order of the 1S_0 contribution. We calculate the contributions of states with $lsj \neq ^1S_0$ crudely by neglecting their orthogonalization to the d + N states. The calculated contributions are shown in Fig. 10. We expect that these contributions are overestimated, and that orthogonalization to d + p states would reduce them. The response obtained by including all the $l=0$ and 1 contributions gives $S_L(k) = 0.90$, while the more accurate ground state calculation¹¹ gives $S_L(k) = 0.92$ at $k = 400$ MeV/c. If the contribution of $l=2$ states is also included, the $S_L(k)$ becomes ~ 0.99 , i.e., it is overestimated by $\sim 7\%$. This essentially means that the contribution of 3N states with $lsj = ^3S_1, ^3P_0, ^3P_1, ^3P_2,$ and 1P_1 has been overestimated enough to compensate that of states with $l \geq 2$. Hence we truncate the sum over l at $l=1$ for ^3He . In the case of ^3H , where the d + n contribution to the $S_L(k, \omega)$ is relatively smaller, we have to include contributions from 3N states having $l=0, 1,$ and 2 to obtain reasonable values of $S_L(k)$.

The statistical error in the Monte Carlo calculation of the matrix elements of $e^{-i\mathbf{k}\cdot\mathbf{R}}\rho_{p,k}$ (Appendix C) introduces an error in the theoretical $S_L(k, \omega)$. This error is negligible in the region of the quasi-elastic peak; however, it grows with increasing energy loss ω . Hence we truncate the microscopic calculation of $S_L(k, \omega)$ at $\omega = \omega_m$, where the statistical error is $\sim 10\%$. The value of ω_m is marked on all the figures.

At $\omega = \omega_m$ the calculated response is larger than that obtained from the impulse approximation:

$$S_{L, \text{IA}}(k, \omega) = \int \frac{d^3k'}{(2\pi)^3} n_p(k') \delta \left[\omega - \frac{\hbar^2 k^2}{2m} - \frac{\hbar^2 \mathbf{k} \cdot \mathbf{k}'}{m} \right], \quad (4.21)$$

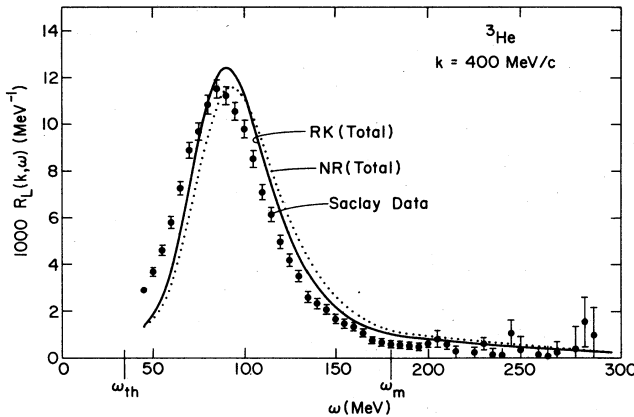


FIG. 9. The total response obtained with CO states and relativistic (solid line labeled RK) and nonrelativistic (dotted line labeled NR) kinematics. See caption of Fig. 7 for other details.

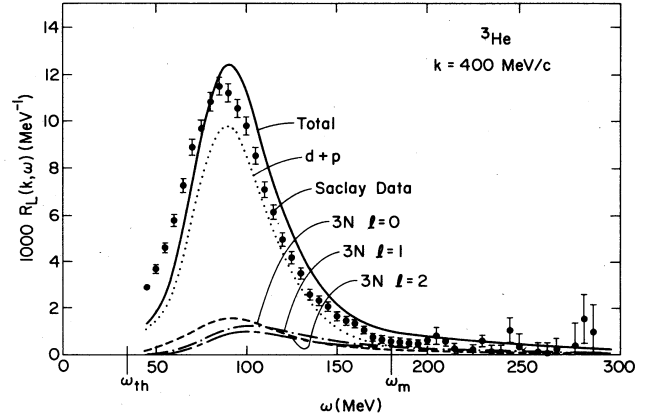


FIG. 10. The contributions of d + p and 3N states with $l=0, 1,$ and 2 to the response of ^3He at $k = 400$ MeV/c. See caption of Fig. 7 for other details.

TABLE I. $S_L(k)$ and $W_L(k)$ of ${}^3\text{He}$ at $k=400$ MeV/c.

ω_m	$S_L(k)$	$\Delta S_L(k)$	$W_L(k)$	$\Delta W_L(k)$
180	0.90	0.07	98.7	17.2
225	0.91	0.05	100.5	12.4

where $n_p(k')$ is the momentum distribution of protons in the ground state. However, we obtain an $S_L(k, \omega)$ that is quite smooth at $\omega = \omega_m$ by assuming that

$$S_L(k, \omega > \omega_m) = c S_{L, \text{IA}}(k, \omega), \quad (4.22)$$

$$c = S_L(k, \omega_m) / S_{L, \text{IA}}(k, \omega_m). \quad (4.23)$$

The $S_L(k)$ and the energy weighted sum $W_L(k)$,

$$W_L(k) = \frac{1}{Z} \int_{\omega_{\text{el}}^+}^{\infty} S_L(k, \omega) \omega d\omega, \quad (4.24)$$

are calculated with the approximate tail (4.22) for $\omega > \omega_m$. This approximation is somewhat *ad hoc*; however, since ω_m is quite large, it is not very important. For example the total values of $S_L(k)$ and $W_L(k)$ for ${}^3\text{He}$ at $k=400$ MeV/c are compared with tail contributions $\Delta S_L(k)$ and $\Delta W_L(k)$ for $\omega_m = 180$ and 225 MeV in Table I.

V. RESULTS

A. The longitudinal response of ${}^3\text{He}$

The response calculated with correlated orthogonal states at $k=300, 400, 500,$ and 600 MeV/c is shown in Figs. 11–14. These figures also show the experimental data from Saclay,¹ and the response obtained in impulse approximation (IA) using the proton and d + p momentum distributions in the ground state.¹⁰ The variational wave function of Ref. 10 is used for the ground state in these calculations.

We note that the response obtained with the CO states is in significantly better agreement with the experimental data than that with the IA. As mentioned in the preceding section, both orthogonalization of the final states and short range correlations in the final states reduce the response in the quasi-free peak. At lower values of k orthogonalization has the more dominant effect. At $k=300$ and 400 MeV/c the peak of the theoretical response is at slightly higher energy as compared with experiment, while the lowest order CO states theory seems to work much better at $k=500$ and 600 MeV/c.

As mentioned earlier, the sums $S_L(k)$ and $W_L(k)$ of the response have been calculated exactly from the

ground state.^{11,12} In Table II we compare the sums calculated from the CO response with the more reliable ground state (g.s.) calculation results, and the $S_L(k)$ deduced from experimental data.^{1,12} Note that the agreement between the CO and g.s. $S_L(k)$ is not meaningful because the sum over l in 3N states is truncated by matching these. However, a comparison of the CO and g.s. $W_L(k)$ is meaningful. It suggests that higher order corrections to the CO calculation will shift the response to lower energies and improve agreement with experiment.

Lastly, we note that the contributions of the d + p states and 3N states with $lsj = {}^1S_0$ account for $\sim 80\%$ of the response. These contributions are calculated with reasonable accuracy in the present work.

B. The longitudinal response of ${}^3\text{H}$

The results obtained for ${}^3\text{H}$ are given in Figs. 15–18. The contributions of d + n states and 3N states with $lsj = {}^1S_0$ account for less than half of the total CO response. Thus these results may be less accurate than those for ${}^3\text{He}$. However, it can also be argued that the corrections from orthogonalizing the 3N states with $lsj \neq {}^1S_0$ to the d + n states, which are neglected in the present work, may not be very important for ${}^3\text{H}$, because the d + n contribution to the response is small. The sums obtained with CO response are in reasonable agreement with the g.s. calculations^{11,12} (Table III), and therefore the present calculation of the ${}^3\text{H}$ response may not be too bad.

We note that the response of ${}^3\text{H}$ is much smaller in the quasi-free peak region than that given by the IA, and it is broader than that of ${}^3\text{He}$. The ${}^3\text{He}$ response shown in Figs. 15–18 has been divided by 2 to account for the difference in the charges of ${}^3\text{H}$ and ${}^3\text{He}$. We hope that the experimental $R_L(k, \omega)$ will soon be available from data taken at Bates.²³

VI. CONCLUSIONS

The longitudinal response of ${}^3\text{He}$, obtained with the lowest-order theory using correlated orthogonal states, has a reasonably correct sum and energy weighted sum, and it is also quite similar to that seen experimentally. There are, however, systematic differences between the calculated and experimental response. For example, at small ω , near the d + N threshold the experimental response is always much larger than the theoretical one. The response in this region is due to states with small value of $|\mathbf{q}|$ for which our correlated state $|2, Q\rangle$ may not be very accurate. The present $|2, Q\rangle$ states are ob-

TABLE II. Sums of longitudinal response of ${}^3\text{He}$.

k (MeV/c)	$S_L(k)$			$W_L(k)$ (MeV)	
	CO	g.s.	Expt.	CO	g.s.
300	0.77	0.78	0.75	56.0	52.3
400	0.90	0.92	0.86	98.7	94.1
500	0.96	0.97	0.94	153	143
600	0.97	0.99	0.98	207	196

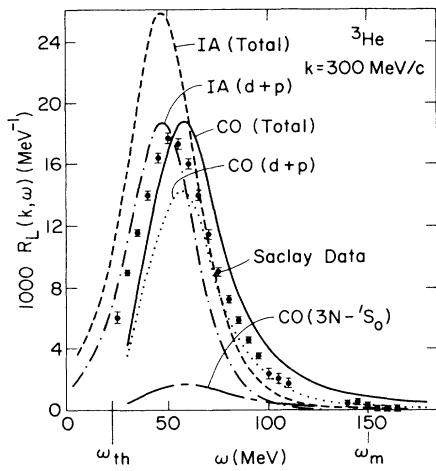


FIG. 11. The total, d + p, and $3N-^1S_0$ response of ^3He at $k = 300 \text{ MeV}/c$ is compared with experiment and the total and d + p response obtained with the impulse approximation.

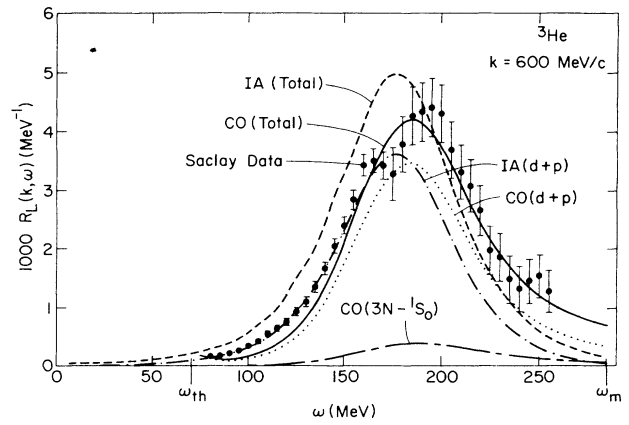


FIG. 14. Same as Fig. 11, but for $k = 600 \text{ MeV}/c$.

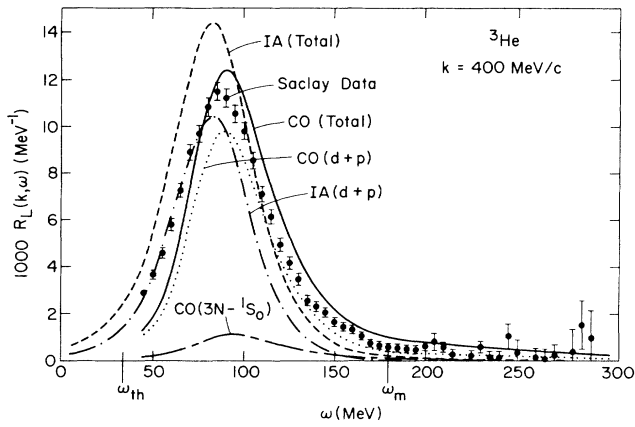


FIG. 12. Same as Fig. 11, but for $k = 400 \text{ MeV}/c$.

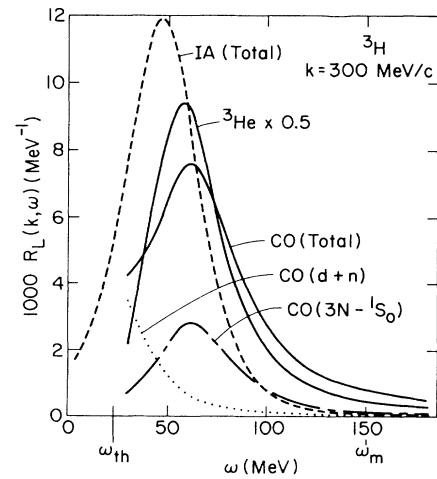


FIG. 15. The total, d + n, and $3N-^1S_0$ response of ^3H is compared with the total response of ^3He divided by 2, and the total response of ^3H obtained in the impulse approximation.

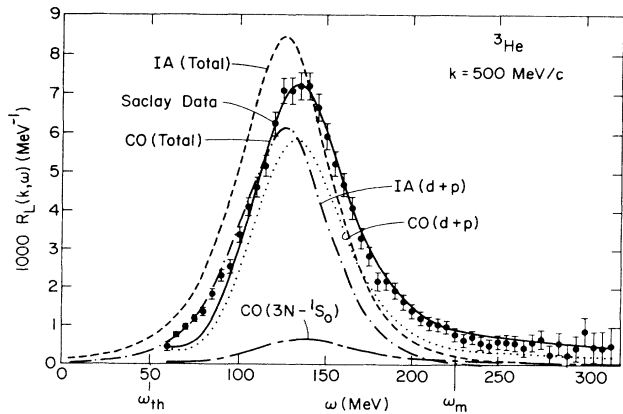


FIG. 13. Same as Fig. 11, but for $k = 500 \text{ MeV}/c$.

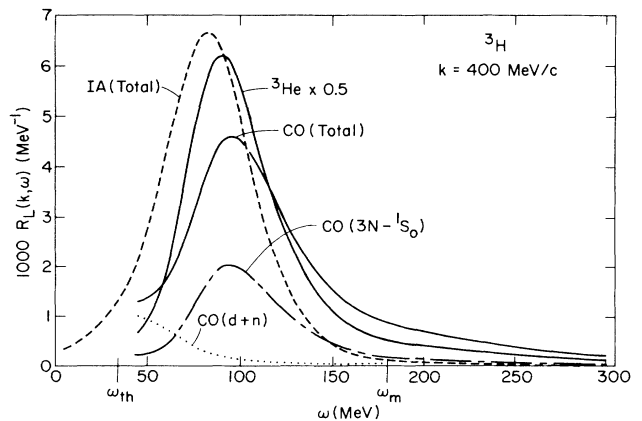
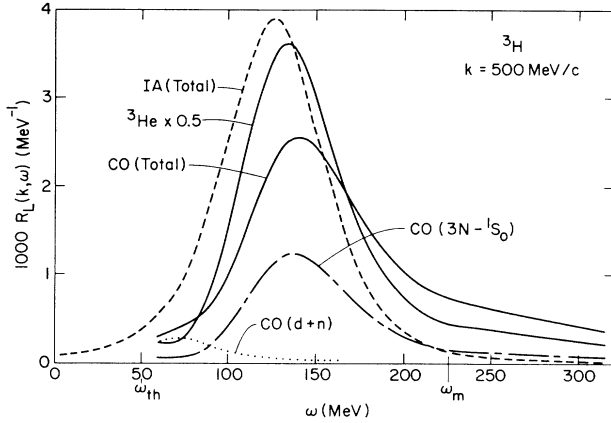
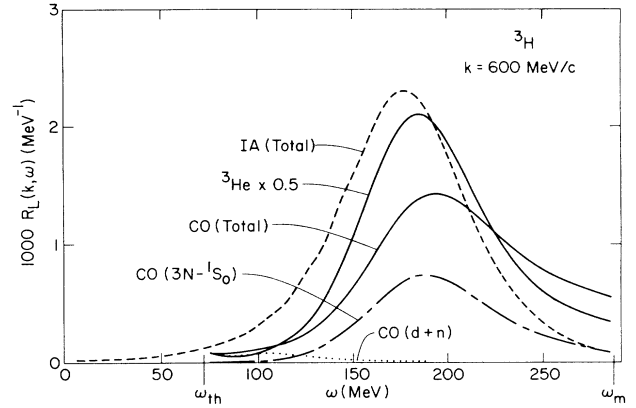


FIG. 16. Same as Fig. 15, but for $k = 400 \text{ MeV}/c$.

FIG. 17. Same as Fig. 15, but for $k = 500$ MeV/c.FIG. 18. Same as Fig. 15, but for $k = 600$ MeV/c.

tained from an uncorrelated state in which the relative motion of the deuteron and the nucleon is described by a plane wave $e^{i\mathbf{q}\cdot(\mathbf{r}_1 - \mathbf{R}_{23})}$. Perhaps it may be more accurate at small values of $|\mathbf{q}|$ to use the real part of the deuteron-nucleon optical potential to calculate this part of the wave function. It may be necessary to make such improvements before attempting a calculation of higher order corrections.

Unlike the calculations of the sums $S_L(k)$ and $W_L(k)$ reported in Refs. 11 and 12, the present calculation of $S_L(k, \omega)$ is not exact. It essentially includes the minimum interaction effects on final state wave functions required to ensure orthogonality and reasonable short range behavior. It is nice that the theory comes quite close to experiment just by including these minimal effects.

It should also be possible to calculate, with the methods developed here, the $S_L(k, \omega)$ of the ${}^4\text{He}$ nucleus. It can be studied experimentally with high accuracy, and the calculated¹² values of $W_L(k)$ suggest that interaction effects are larger in this nucleus.

ACKNOWLEDGMENTS

The authors would like to thank Dr. J. Morgenstern, Dr. C. Marchand, and Professor M. K. Brussel for the data on $R_L(k, \omega)$ of ${}^3\text{He}$. This research has been supported by The U.S. National Science Foundation via Grant PHY84-15064. The calculations reported here were made possible by grant of time on the Cray computer at the National Center for Supercomputer Applications in Urbana, Illinois.

APPENDIX A: THE CORRELATION OPERATOR F_{ij}

Let us consider two nucleons in the relative 1S_0 state. Their wave function,

$$\psi({}^1S_0, \mathbf{r}) = \frac{1}{r} u(k, r) y_{00}^{00}, \quad (\text{A1})$$

where y_{jm}^{ls} is the spin and angle part, is obtained from the solution of the Schrödinger equation,

$$\left[-\frac{\hbar^2}{m} \frac{d^2}{dr^2} + v({}^1S_0, r) \right] u(k, r) = \frac{\hbar^2 k^2}{m} u(k, r), \quad (\text{A2})$$

where $v({}^1S_0, r)$ is the potential in the 1S_0 channel. The radial wave function $(1/r)u(k, r)$ differs from the unperturbed radial wave function $j_0(kr)$ at small r due to the strong $v({}^1S_0, r)$, and at large r due to the phase shift. We want to express the difference between the $(1/r)u(k, r)$ and $j_0(k, r)$ at small r by a multiplicative correlation function $f({}^1S_0, r)$. The ratio of $(1/r)u(k, r)$ and $j_0(kr)$ is not very sensitive to k at small r . The phase shift, on the other hand, depends strongly on k and is calculated perturbatively with correlated states.

Following techniques developed in the theory of nuclear matter,¹⁹ we define a new short-range potential:

$$\bar{v}({}^1S_0, r) = [v({}^1S_0, r) + \lambda({}^1S_0)] \Theta(d_c - r). \quad (\text{A3})$$

Let $\bar{u}(k, r)$ be the solution of the Schrödinger equation for $\bar{v}({}^1S_0, r)$. The $\lambda({}^1S_0)$ is chosen so that

TABLE III. Sums of longitudinal response of ${}^3\text{H}$.

k (MeV/c)	$S_L(k)$		$W_L(k)$ (MeV)	
	CO	g.s.	CO	g.s.
300	0.83	0.83	64.8	64.5
400	0.88	0.94	107	110
500	0.91	0.98	162	162
600	0.93	1.00	232	218

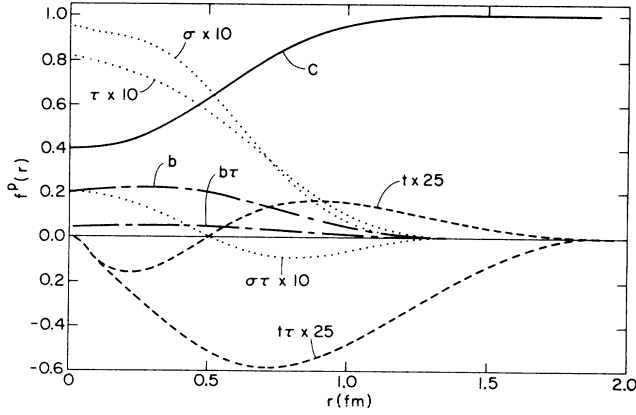


FIG. 19. The central, $\tau_i \cdot \tau_j$, $\sigma_i \cdot \sigma_j$, $\tau_i \cdot \tau_j \sigma_i \cdot \sigma_j$, S_{ij} , $\tau_i \cdot \tau_j S_{ij} L$, $\mathbf{L} \cdot \mathbf{S}$, and $\tau_i \cdot \tau_j \mathbf{L} \cdot \mathbf{S}$ correlations in the F_{ij} are shown by curves labeled c , τ , σ , $\sigma\tau$, t , $t\tau$, b , and $b\tau$, respectively.

$$\frac{1}{r} \bar{u}(k, r > d_c) = j_0(kr) \quad (\text{A4})$$

and

$$f({}^1S_0, r) = \frac{1}{r} \bar{u}(k, r) / j_0(kr), \quad (\text{A5})$$

for some typical value of k . The $f({}^1S_0, r)$ equals one for $r > d_c$ by construction, and it reflects the difference between $(1/r)u(k, r)$ and $j_0(kr)$ at small r where $\lambda({}^1S_0) \ll v({}^1S_0, r)$. The correlation function $f(lsj, r)$ in other uncoupled states like 1P_1 is calculated in a similar way.

Let us now consider two nucleons in the relative 3S_1 state, which is coupled to the 3D_1 state by the tensor force. The Schrödinger equation is solved for the two-body potential:

$$\bar{v}({}^3S_1, r) = [v_{0,1}^c(r) + v_{0,1}^b(r) \mathbf{L} \cdot \mathbf{S} + v_{0,1}^{bb}(r) (\mathbf{L} \cdot \mathbf{S})^2 + v_{0,1}^q(r) L^2 + \lambda^c({}^3S_1)] \Theta(d_c - r) + [v_{0,1}^t(r) + \lambda^t({}^3S_1)] S_{12} \Theta(d_t - r), \quad (\text{A6})$$

where $v_{0,1}^x(r)$ for $x = c; b, bb, q$, and t denote the central, $(\mathbf{L} \cdot \mathbf{S})$, $(\mathbf{L} \cdot \mathbf{S})^2$, L^2 , and tensor potentials in the $t=0$, $S=1$ channel. The solution of the Schrödinger equation has the form

$$\bar{\psi}({}^3S_1, r) = \frac{1}{r} \bar{u}(k, r) y_{1m}^{01} + \frac{1}{r} \bar{w}(k, r) y_{1m}^{21}, \quad (\text{A7})$$

and the $\lambda^c({}^3S_1)$ and $\lambda^t({}^3S_1)$ are chosen so that

$$\frac{1}{r} \bar{u}(k, r > d_c) = j_0(kr), \quad (\text{A8})$$

$$\bar{w}(k, r > d_t) = 0. \quad (\text{A9})$$

The radial and tensor correlations in the 3S_1 state are then obtained as

$$f({}^3S_1, r) = \frac{1}{r} \bar{u}(k, r) / j_0(kr) \quad (\text{A10})$$

and

$$f^t({}^3S_1, r) = \frac{1}{r} \bar{w}(k, r) / [\sqrt{8} j_0(kr)]. \quad (\text{A11})$$

The $f^t({}^3S_1, r > d_t) = 0$ by construction.

The radial correlations in 1S_0 , 3P_0 , 3P_2 , 3S_1 , 3D_3 , and 1P_1 states and the tensor correlations in 3S_1 and 3P_2 states are calculated in this way. These eight correlations are expressed as an operator:

$$F_{ij} = \sum_{p=1,8} f^p(r_{ij}) O_{ij}^p, \quad (\text{A12})$$

where $O_{ij}^{p=1,6}$ are given in Eq. (2.4), and

$$O_{ij}^{p=7,8} = (\mathbf{L} \cdot \mathbf{S}) \text{ and } (\mathbf{L} \cdot \mathbf{S}) \tau_i \cdot \tau_j. \quad (\text{A13})$$

The parameters d_c , d_t , and k chosen for the calculation of F_{ij} have values of 1.4 fm, 1.9 fm, and 0.78 fm^{-1} . This value of k corresponds to $E_{\text{lab}} \sim 50 \text{ MeV}$. The results of this work are not very sensitive to $\sim 20\%$ changes in these parameters. The calculated $f^p(r)$ are shown in Fig. 19. Note that in all the calculations reported here we have used the correlation operator (2.3), in which the spin-orbit correlations $f^{p=7,8}$ are set to zero.

APPENDIX B: CALCULATION OF NN SCATTERING

The plane waves $e^{i\mathbf{k} \cdot \mathbf{r}} |sm_s tm_t\rangle$ are expanded into partial waves:

$$e^{i\mathbf{k} \cdot \mathbf{r}} |sm_s tm_t\rangle = 4\pi \sum_{jm_j l} (i)^l j_l(kr) [Z_{lsm_s}^{jm_j}(\hat{\mathbf{k}})]^* y_{jm_j}^{ls} |tm_t\rangle, \quad (\text{B1})$$

$$Z_{lsm_s}^{jm_j}(\hat{\mathbf{k}}) \equiv \sum_{m_l} \langle lm_l sm_s | jm_j \rangle Y_{lm_l}(\hat{\mathbf{k}}). \quad (\text{B2})$$

The CBBA T matrix is given by

$$T(\mathbf{k}m_s, \mathbf{k}'s'm'_s; t) = (4\pi)^2 \sum_{jm, l'l'} (i)^{l-l'} [1 - (-1)^{l+s+t}] Z_{l'sm'_s}^{jm_j}(\hat{\mathbf{k}}') [Z_{lsm_s}^{jm_j}(\hat{\mathbf{k}})]^* H_{l'l}^{jts}(k), \quad (\text{B3})$$

$$H_{l'l}^{jts}(k) \equiv \left\langle j_{l'}(kr) y_{jm'_j}^{l's'} t m_t \left| F^\dagger \left[v - \frac{\hbar^2}{m} (\nabla^2 - k^2) \right] F \left| j_l(kr) Y_{jm_j}^{ls} t m_t \right. \right\rangle, \quad (\text{B4})$$

where we have used $k' = k$. The operators $F^\dagger v F$ and $F^\dagger \nabla^2 F$ are easy to calculate, as discussed in Ref. 19. The differential cross section in the center of mass (c.m) frame, for nn scattering, is given by

$$\frac{d\sigma_{nn}}{d\Omega}(\mathbf{k}m_s, \mathbf{k}'m'_s, s) = \left[\frac{m}{4\pi\hbar^2} \right]^2 |T(\mathbf{k}sm_s, \mathbf{k}'sm'_s; t = 1)|^2, \quad (\text{B5})$$

while that for np scattering is

$$\frac{d\sigma_{np}}{d\Omega}(\mathbf{k}m_s, \mathbf{k}'m'_s, s) = \frac{1}{4} \left[\frac{m}{4\pi\hbar^2} \right]^2 |T(\mathbf{k}sm_s, \mathbf{k}'sm'_s; t = 0) + T(\mathbf{k}sm_s, \mathbf{k}'sm'_s; t = 1)|^2. \quad (\text{B6})$$

In the calculations reported here we have retained all terms having $j \leq 5$. The spin averaged cross sections shown in Figs. 1–6 are defined as

$$\frac{d\sigma}{d\Omega} = \frac{1}{4} \left[\frac{d\sigma}{d\Omega}(\mathbf{k}, \mathbf{k}', s = 0) + \sum_{m_s, m'_s} \frac{d\sigma}{d\Omega}(\mathbf{k}m_s, \mathbf{k}'m'_s, s = 1) \right]. \quad (\text{B7})$$

APPENDIX C: CALCULATION OF MATRIX ELEMENTS AND OVERLAPS

1. Calculation of

$$\langle n, Q | e^{-i\mathbf{k}\cdot\mathbf{R}} \rho_{p,\mathbf{k}} - F_{el}(\mathbf{k}, M_S M_T) | 1, M_S M_T \rangle$$

These matrix elements are calculated with the Monte Carlo method discussed in Ref. 10. The variational wave function of the three-nucleon ground state is written as

$$|n, Q\rangle = \frac{1}{\sqrt{3}} \sum_{\text{cyc}} f^c(r_{12}) f^c(r_{13}) \frac{1}{2} \{U_2(12), U_2(13)\} e^{i\mathbf{q}\cdot(\mathbf{r}_1 - \mathbf{R}_{23})} \chi_\alpha(1) \phi_{E_2\gamma}(23). \quad (\text{C4})$$

The matrix element is written as

$$\langle n, Q | e^{-i\mathbf{k}\cdot\mathbf{R}} \rho_{p,\mathbf{k}} - F_{el}(\mathbf{k}, M_S M_T) | 1, M_S M_T \rangle = \sqrt{3} \int d\mathbf{r}_1 d\mathbf{r}_2 d\mathbf{r}_3 W(\mathbf{r}_1, \mathbf{r}_2, \mathbf{r}_3) X(\mathbf{k}, n, Q). \quad (\text{C5})$$

$$W(\mathbf{r}_1, \mathbf{r}_2, \mathbf{r}_3) = f^c(r_{12}) f^c(r_{13}) f_3^c(r_{12}) f_3^c(r_{23}) f_3^c(r_{31}), \quad (\text{C6})$$

$$X(\mathbf{k}, n, Q) = \chi_\alpha^\dagger(1) \phi_{E_2\gamma}^\dagger(23) e^{-i\mathbf{q}(\mathbf{r}_1 - \mathbf{R}_{23})} \frac{1}{2} \{U_2(12), U_2(13)\} [e^{-i\mathbf{k}\cdot\mathbf{R}} \rho_{p,\mathbf{k}} - F_{el}(\mathbf{k}, M_S M_T)] U_3 \Phi_3(M_S M_T), \quad (\text{C7})$$

and evaluated with the Monte Carlo method by using $W(\mathbf{r}_1, \mathbf{r}_2, \mathbf{r}_3)$ as the weight function. We used 75 000 configurations to calculate the matrix elements with $d + N$ states and $3N$ states with $l = 0$, and 18 750 configurations for $3N$ states with $l = 1$ and 2.

$$|1, M_S M_T\rangle = \left[\prod_{i < j \leq 3} f_3^c(ij) \right] U_3 \Phi_3(M_S M_T), \quad (\text{C1})$$

$$U_3 = S \prod_{i < j \leq 3} \left[1 + \sum_p f_{ij}^p u_3^p(r_{ij}) O_{ij}^p \right], \quad (\text{C2})$$

given in Eq. (2.3) of Ref. 10. We use f_3^c and u_3^p to denote correlations in the ground state. These functions are also given in Ref. 10 along with the three-nucleon functions f_{ij}^p .

The correlation operator F in the continuum states $|n, Q\rangle$ is written as

$$F_{ij} = f^c(r_{ij}) \left[1 + \sum_{p=2,6} u^p(r_{ij}) O_{ij}^p \right] \\ \equiv f^c(r_{ij}) U_2(ij), \quad (\text{C3})$$

and the states $|n, Q\rangle$ then have the form

2. Calculation of the overlaps

The overlaps $(2, \mathbf{q}\sigma_z M_d | 2, \mathbf{q}'\sigma'_z M'_d)$ and $(2, \mathbf{q}\sigma_z M_d | 1, M_S M_T)$ are needed to calculate the Löwdin corrections to the $d + N$ part of the response [Eqs. (4.10)–(4.12)]. These matrix elements are easily calculated with the approximation $F=1$. In this case $(2, \mathbf{q}\sigma_z M_d | 1, M_S M_T)$ becomes the amplitude for finding a deuteron and a nucleon with momentum \mathbf{q} in the three-nucleon ground state. These amplitudes are calculated in Ref. 10.

Approximating $F=1$, we obtain

$$(2, \mathbf{q}\sigma_z M_d | 2, \mathbf{q}'\sigma'_z M'_d) \approx \langle \mathbf{q}(1, 23)\sigma_z(1)\tau_z(1)\phi_{M_d}(23) | \sum_{\text{cyc}} \mathbf{q}'(i, jk)\sigma'_z(i)\tau_z(i)\phi_{M'_d}(jk) \rangle \quad (\text{C8})$$

$$= 2 \langle \sigma_z(1)\tau_z(1)\tilde{\phi}_{M_d}(\mathbf{q}' + \mathbf{q}/2, 23) | \sigma'_z(2)\tau_z(2)\tilde{\phi}'_{M'_d}(\mathbf{q}'/2 + \mathbf{q}, 31) \rangle, \quad (\text{C9})$$

where $\mathbf{q}(i, jk)$ stands for $e^{i\mathbf{q}\cdot(\mathbf{r}_i - \mathbf{R}_{jk})}$ and $\tilde{\phi}_{M_d}(\mathbf{k}, ij)$ is the deuteron wave function in momentum space,

$$\tilde{\phi}_{M_d}(\mathbf{k}, ij) = [\tilde{u}(k)y_{1M_d}^{01}(\hat{\mathbf{k}}, ij) + \tilde{w}(k)y_{1M_d}^{21}(\hat{\mathbf{k}}, ij)], \quad (\text{C10})$$

Here and in the rest of this appendix we suppress isospin functions for brevity.

The two-nucleon wave function $\phi(p, lsm_j)$ in the 3N states has the form

$$\phi(p, lsm_j) = \frac{1}{r} u(p, lsj, r)y_{lm_j}^{ls}(\hat{\mathbf{r}}), \quad (\text{C11})$$

$$u(p, lsj, r \rightarrow \infty) = \frac{1}{p} \sin \left[pr - \frac{l\pi}{2} + \delta_{lsj}(p) \right], \quad (\text{C12})$$

for uncoupled channels like $lsj = {}^1S_0$. For coupled channels like 3S_1 , where $j = l + 1$,

$$\phi(p, lsm_j) = \frac{1}{r} u(p, lsj, r)y_{lm_j}^{ls}(\hat{\mathbf{r}}) + \frac{1}{r} w(p, l'sj, r)y_{lm_j}^{l's}(\hat{\mathbf{r}}), \quad (\text{C13})$$

and $l' = l + 2$. The asymptotic forms of u and w are

$$u(p, lsj, r \rightarrow \infty) = \frac{1}{p} \cos[\epsilon_j(p)] \sin \left[pr - \frac{l\pi}{2} + \delta_{lsj}(p) \right], \quad (\text{C14})$$

$$w(p, l'sj, r \rightarrow \infty) = \frac{1}{p} \sin[\epsilon_j(p)] \sin \left[pr - \frac{l'\pi}{2} + \delta_{lsj}(p) \right], \quad (\text{C15})$$

where $\delta_{lsj}(p)$ are the phase shifts and $\epsilon_j(p)$ are the mixing angles.

Since the corrections from orthogonalizing the 3N states to the $d + N$ states have been studied only for the case $lsj = {}^1S_0$, we discuss only this simple case. The Fourier transform of $\phi(p, {}^1S_0)$ is calculated by isolating the asymptotic part of $u(p, {}^1S_0)$:

$$u(p, {}^1S_0) = u_{\text{asy}}(p, {}^1S_0) + u_s(p, {}^1S_0), \quad (\text{C16})$$

$$u_{\text{asy}}(p, {}^1S_0) = \cos\delta_0(p)rj_0(pr) - \sin\delta_0(p)rn_0(pr), \quad (\text{C17})$$

where $\delta_0(p)$ is the 1S_0 phase shift. The $u_s(p, {}^1S_0)$ is a short ranged wave function whose Fourier transform $\tilde{u}_s(k, p, {}^1S_0)$ is not singular. We obtain

$$\begin{aligned} \tilde{\phi}(k, p, {}^1S_0) = & \left[2\pi^2 \cos\delta_0(p) \frac{\delta(k-p)}{kp} \right. \\ & + 4\pi \sin\delta_0(p) \frac{1}{p} \mathcal{P} \frac{1}{k^2 - p^2} \\ & \left. + \tilde{u}_s(k, p, {}^1S_0) \right] y_{00}^{00}, \quad (\text{C18}) \end{aligned}$$

where \mathcal{P} denotes the Cauchy principal value. In the $F=1$ approximation we obtain

$$(3, \mathbf{q}\sigma_z p {}^1S_0 | 2, \mathbf{q}'\sigma'_z M'_d) = 2 \langle \sigma'_z(1)\tilde{\phi}(\mathbf{q}' + \mathbf{q}/2, p, {}^1S_0, 23) | \sigma'_z(2)\tilde{\phi}'_{M'_d}(\mathbf{q}'/2 + \mathbf{q}, 31) \rangle. \quad (\text{C19})$$

The overlap,

$$(3, \mathbf{q}\sigma_z p {}^1S_0 | 1, M_S) \approx \sqrt{3} \int d\mathbf{r}_1 d\mathbf{r}_2 d\mathbf{r}_3 \sigma_z^\dagger(1)\phi^\dagger(p, {}^1S_0, 23)e^{-i\mathbf{q}\cdot(\mathbf{r}_1 - \mathbf{R}_{23})}\psi_{3, M_S}, \quad (\text{C20})$$

is calculated by the Monte Carlo method of Ref. 10. The overlap matrix element in Eq. (4.17) is then approximated as

$$(3, \mathbf{q}\sigma_z p {}^1S_0 | 2, \mathbf{q}'\sigma'_z M'_d) \approx (3, \mathbf{q}\sigma_z p {}^1S_0 | 2, \mathbf{q}'\sigma'_z M'_d) \quad (\text{C21})$$

$$= (3, \mathbf{q}\sigma_z p {}^1S_0 | 2, \mathbf{q}'\sigma'_z M'_d) - \sum_{M_S} (3, \mathbf{q}\sigma_z p {}^1S_0 | 1, M_S)(1, M_S | 2, \mathbf{q}'\sigma'_z M'_d), \quad (\text{C22})$$

and all the matrix elements in (C22) are calculated as discussed above in the approximation $F=1$.

- ¹C. Marchand *et al.*, Phys. Lett. **153B**, 29 (1985); CEN Saclay Report CEA-N-2439, 1985; J. Morgenstern, private communication.
- ²P. Barreau *et al.*, Nucl. Phys. **A402**, 515 (1983).
- ³Z. E. Meziani *et al.*, Phys. Rev. Lett. **52**, 2130 (1984).
- ⁴M. Dedy *et al.*, Phys. Rev. C **33**, 1987 (1986).
- ⁵C. C. Blatchley *et al.*, Phys. Rev. C **34**, 1243 (1986).
- ⁶K. Bätzner *et al.*, Phys. Lett. **39B**, 575 (1972).
- ⁷J. V. Noble, Phys. Rev. Lett. **46**, 412 (1981).
- ⁸C. M. Shakin, Nucl. Phys. **A446**, 323c (1985).
- ⁹C. R. Chen *et al.*, Phys. Rev. C **33**, 1740 (1986).
- ¹⁰R. Schiavilla, V. R. Pandharipande, and R. B. Wiringa, Nucl. Phys. **A449**, 219 (1986).
- ¹¹R. Schiavilla *et al.*, Nucl. Phys. **A473**, 267 (1987).
- ¹²R. Schiavilla, A. Fabrocini, and V. R. Pandharipande, Nucl. Phys. **A473**, 290 (1987).
- ¹³H. Meier-Hajduk *et al.*, Nucl. Phys. **A395**, 332 (1983).
- ¹⁴J. M. Laget, Phys. Lett. **151B**, 325 (1985).
- ¹⁵E. Feenberg, *Theory of Quantum Fluids* (Academic, New York, 1969).
- ¹⁶S. Fantoni and V. R. Pandharipande, Nucl. Phys. **A473**, 234 (1987).
- ¹⁷J. V. Noble, Phys. Rev. C **17**, 2151 (1978).
- ¹⁸J. M. Eisenberg, J. V. Noble, and H. J. Weber, Phys. Rev. C **19**, 276 (1979).
- ¹⁹V. R. Pandharipande and R. B. Wiringa, Rev. Mod. Phys. **51**, 821 (1979).
- ²⁰P. O. Löwdin, J. Chem. Phys. **18**, 365 (1950).
- ²¹R. B. Wiringa, R. A. Smith, and T. L. Ainsworth, Phys. Rev. C **29**, 1207 (1984).
- ²²C. Ciofi degli Atti, Prog. Part. Nucl. Phys. **3**, 163 (1980).
- ²³K. Dow, private communication.